ACS APPLIED MATERIALS & INTERFACES

Research Article

www.acsami.org

Corrugated Paraffin Nanocomposite Films as Large Stroke Thermal Actuators and Self-Activating Thermal Interfaces

Davor Copic[†]

Department of Mechanical Engineering, University of Michigan, 2350 Hayward Street, Ann Arbor, Michigan 48109, United States

A. John Hart*

Department of Mechanical Engineering and Laboratory for Manufacturing and Productivity, Massachusetts Institute of Technology, 77 Massachusetts Avenue, Cambridge, Massachusetts 02139, United States

Department of Mechanical Engineering, University of Michigan, 2350 Hayward Street, Ann Arbor, Michigan 48109, United States

Supporting Information

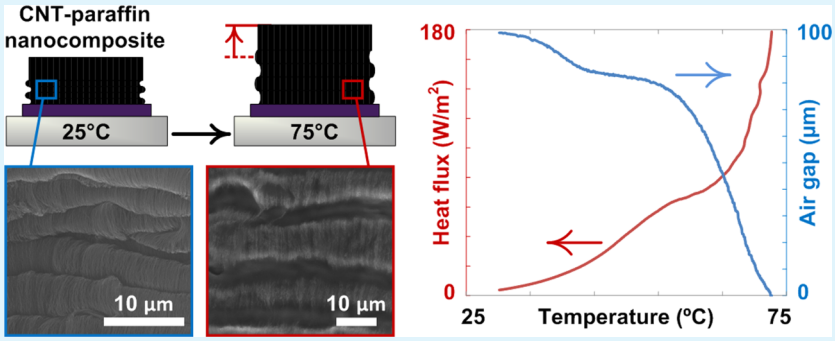

ABSTRACT: High performance active materials are of rapidly growing interest for applications including soft robotics, microfluidic systems, and morphing composites. In particular, paraffin wax has been used to actuate miniature pumps, solenoid valves, and composite fibers, yet its deployment is typically limited by the need for external volume constraint. We demonstrate that compact, high-performance paraffin actuators can be made by confining paraffin within vertically aligned carbon nanotube (CNT) films. This large-stroke vertical actuation is enabled by strong capillary interaction between paraffin and CNTs and by engineering the CNT morphology by mechanical compression before capillary-driven infiltration of the molten paraffin. The maximum actuation strain of the corrugated CNT-paraffin films (~0.02−0.2) is comparable to natural muscle, yet the maximum stress is limited to ~10 kPa by collapse of the CNT network. We also show how a CNT−paraffin film can serve as a self-activating thermal interface that closes a gap when it is heated. These new CNT−paraffin film actuators could be produced by large-area CNT growth, infiltration, and lamination methods, and are attractive for use in miniature systems due to their self-contained design.

KEYWORDS: *active material, thermal interface, nanocomposite, carbon nanotube, mechanics*

INTRODUCTION

Continued development of active materials whose dimensions can be changed using electrical, optical, or thermal stimuli is essential to advancing applications such as robotic manipulators, shape-changing composites, and microfluidic pumps and valves. Specifically, paraffin wax has found longstanding use in linear actuators with centimeter-scale and larger dimensions, which are widely used in automotive and aerospace systems. This is because paraffin wax exhibits a large and repeatable volume change (10−40%) and stress output (10−100 MPa)[1,2] upon melting, which results in a high mechanical energy density (10^7 J m^{-3})[2] (Figure S1, Supporting Information). However, paraffin-based actuators are found to exhibit noticeably smaller actuation strains and stresses when compared to standard pressure−volume−temperature (PVT) data. For example, Kabei et al. have shown a paraffin actuator capable of reaching strains up to 6% under 2 MPa of load. In comparison to paraffin, thin film shape memory alloy (SMA) actuators exhibit actuations strains of 7×10^{-3}−7×10^{-2} and stresses of 100−700 MPa, while thin film piezoelectric (PZT) actuators exhibit actuation strains of 5×10^{-6}−2×10^{-4} and stresses of 1−9 MPa.[3] Because figures of merit, such as maximum actuation strain and stress, cannot be arbitrarily combined, maximum actuation strain usually corresponds to a zero load condition.

Received: February 6, 2015
Accepted: March 30, 2015
Published: March 30, 2015

DOI: 10.1021/acsami.5b01141
ACS Appl. Mater. Interfaces 2015, 7, 8218−8224

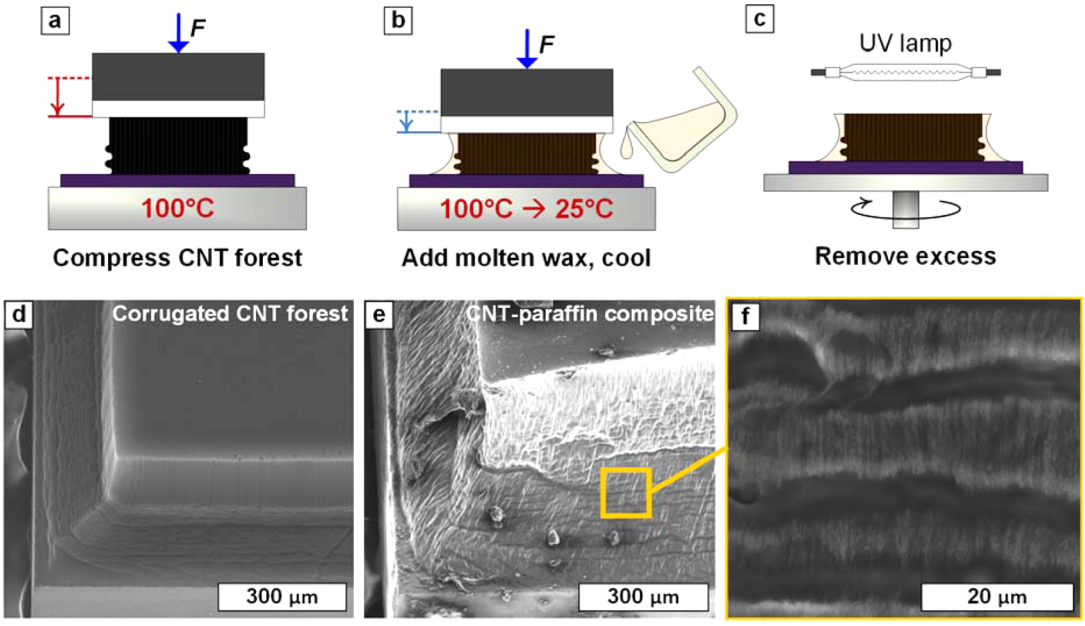

Figure 1. Fabrication of corrugated CNT−paraffin nanocomposite films: (a−c) Key process steps; SEM images of (d) compressed CNT forest with corrugations and (e) CNT−paraffin composite film, with (f) close-up of corrugated microstructure.

Paraffin has also been incorporated in microscale systems including on-chip pumps,[4] valves,[5−8] thin-film cantilevers,[5,9] and linear actuators.[10] Odgen et al. recently reviewed the design and performance of miniaturized paraffin actuators, valves, and pumps.[11] These designs and the related fabrication methods are complicated by the need to confine the paraffin during melting, which is needed to convert the expansion of the paraffin wax into a directed motion. As a result, the overall system performance of miniature paraffin actuators is often compromised relative to the intrinsic actuation capability of paraffin. These actuators also require a large footprint compared to the size of active material used.

Therefore, owing to its intrinsic performance and simplicity of operation, it would be useful to develop more scalable means to harness the actuation capability of paraffin wax in composite materials. Recently, Lima et al. demonstrated microfiber actuators that comprised carbon nanotube (CNT) yarns infiltrated with paraffin wax.[12,13] In these actuators, the wax melts inside the yarn upon heating and remains confined within the yarn due to its strong wetting of the CNTs and high surface tension. As the wax expands, it swells the CNT yarn, which causes the composite to contract its length due to the mechanical anisotropy introduced by the twist of the CNTs about the yarn axis. These yarns exhibited up to 8% contraction upon heating[12] and were able to lift 17 700 times their own weight with a 3% axial contraction.

In this paper, we show how large stroke thin film nanocomposite actuators can be made by confining paraffin within vertically aligned CNT films (CNT "forests") and how the actuation stroke of the composite can be engineered by corrugating the forests on the microscale. We find that actuation is governed by two distinct regimes of operation: (1) low strain expansion below the wax melting point, wherein the composite actuator has high stiffness and (2) high strain expansion during and beyond the melting transition, wherein the actuator has much lower stiffness. Last, we show how the high strain regime can be exploited to build a self-activating thermal interface, where the vertical extension of the nanocomposite film causes it to contact a second substrate, resulting in enhanced heat dissipation at elevated temperature.

RESULTS AND DISCUSSION

CNT−paraffin nanocomposite films were fabricated by capillary driven infiltration of molten paraffin wax into vertically aligned CNT forests, as shown in Figure 1. First, CNT forests were grown on silicon wafers by atmospheric pressure thermal chemical vapor deposition (CVD) using a supported catalyst (1/10 nm Fe/Al_2O_3) deposited by sputtering (see Methods section, Supporting Information).[14,15] After the allotted growth time, which determines the CNT forest height, the CVD system was cooled rapidly while the hydrocarbon flow was maintained; this resulted in strong CNT−substrate adhesion, which prevented delamination of the forest during paraffin expansion.

Next, the CNT forest was compressed vertically using a precision actuator while resting on a hot plate. Upon compression, the CNTs collectively folded, starting at the base of the forest, which resulted in the corrugated morphology shown in Figure 1, panel D.[16−19] The corrugated morphology is visually reminiscent of a macroscopic accordion bellows. Unless otherwise noted below, the CNT forest was compressed to 50% of its as-grown height. Next, the corrugated CNT forest was heated to 100 °C, and molten paraffin wax was poured onto to the sample from the side, while the compressive load was maintained. The wax rapidly wetted the CNTs and wicked into the forest. The hot plate was then cooled (~4 °C/min) to 35 °C, while the sample was kept under constant load. Under constant load, the CNT forest initially shrinks upon wax infiltration and then shrinks further upon cooling. Last, the wax-infiltrated CNT forest was removed from the hot plate and placed on a spin-coater. The sample was heated using a UV lamp, which caused the wax to melt, and spinning was used to remove excess wax from the substrate while the wax was retained within the CNT forest due to capillary action.

The corrugated forest morphology is essential to achieving large actuation stroke upon paraffin phase change. Maintaining

DOI: 10.1021/acsami.5b01141
ACS Appl. Mater. Interfaces 2015, 7, 8218−8224

compressive load during paraffin infiltration and cooling allows the corrugated morphology to be maintained in the nanocomposite film. If the CNT forest is unloaded before paraffin infiltration, the wave-like corrugation is only partially recovered because the elastic energy stored in the deformed CNTs is counteracted by the van der Waals adhesion between CNT contacts created during forest compression. If the forest is infiltrated with paraffin without maintaining the compressive load, the forest expands to approximately 80% of its initial height during cooling and develops cracks in its top surface during cooling (Figure S2, Supporting Information). These cracks, which extend through to the substrate, are caused by local capillary aggregation of the CNTs, which is driven by the shrinkage of the wax upon cooling. The pressure from capillary aggregation exceeds the lateral strength of the forest and causes these cracks. Upon thermal cycling, such cracked composite films close and open their cracks, instead of expanding and contracting vertically, and therefore do not operate as intended.

Upon heating, the crack-free nanocomposite film expands vertically, and the wavelength of the corrugations increases, visually resembling inflation of an accordion bellows. A side view optical image at 25 °C and a mirrored image of the same film heated to 150 °C are shown in Figure 2, panel A. Measurements of the thermally induced strain with no load applied were made via edge tracking of optical images taken using a telecentric lens backlit by a collimated white light source. This actuator extended vertically by ∼17% (perpendicular to the substrate) at 150 °C, as shown in Video S3 of the Supporting Information. Strain versus temperature data from three consecutive heating and cooling cycles (Figure 2B) show that the vertical actuation of the nanocomposite is repeatable. In further experiment, we cycled the actuators up to 10 times without observing degradation. Further work is certainly needed to investigate the durability and identify means to prevent long-term degradation especially when operated in air.

With increasing temperature below the melting point, the CNT−paraffin film expands slowly, then it expands rapidly through the melting transition (53−57 °C), and after that it expands in an approximately linear relationship with temperature. Thus, the strain−temperature curve of a characteristic CNT−paraffin actuator has three distinct regions: (1) low thermal expansion below the melting point, (2) rapid expansion during melting, and (3) further expansion driven by the increased pressure of the confined molten wax. In the second and third regions, the shape of the curve for the CNT−paraffin nanocomposite is similar to that for unconstrained paraffin wax of similar molecular weight[20] but exhibits a lower volume change. Through the complete thermal cycle, the CNT−paraffin films undergo a volume change of approximately 20%. Although the generated change in volume compares favorably to other paraffin based actuators, standard PVT[20] data for unconstrained neat paraffin wax of similar molecular weight exhibit a volume increase of approximately 40%. In practice, all paraffin actuators exhibit less than 40% volume change because the wax must be confined to extract any useful work. In our case, paraffin does work against the stiffness of the CNT forest to expand the composite. Comparable mechanisms limit the strain of macroscale paraffin actuators, yet to a greater degree, wherein the paraffin is held within a container. For further discussion, we denote the low thermal expansion region below the melting point as "regime 1" and the subsequent behavior of rapid expansion upon melting and linear expansion beyond melting as "regime 2".

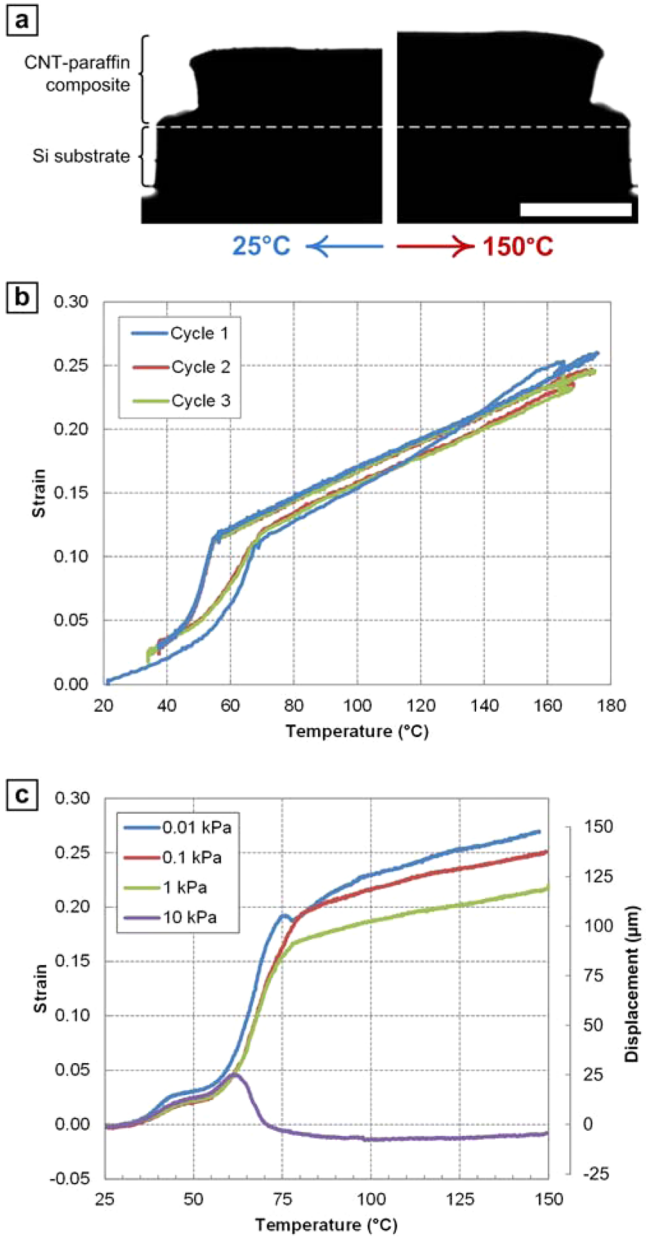

Figure 2. Actuation of CNT−paraffin composite films. (a) Image of the actuator side view at 25 °C and a mirrored image of the same view at 150 °C with 1 mm scale bar. (b) Three consecutive cycles of a CNT−paraffin actuator under no load. (c) Displacement and strain versus temperature under varying values of constant applied stress during heating.

To explore the underlying actuation mechanism of each regime and the relationship between applied force and actuation strain, we applied constant loads during heating while monitoring the vertical displacement of the film, using a feedback-controlled loading system. Consecutive thermal strain curves under constant stress levels varying by factors of 10, from 0.01−10 kPa, are shown in Figure 2, panel C. In regime 1 (below the wax melting point), all four strain curves overlap closely and reach a maximum thermal strain of 3% at 50 °C. For all but the 10 kPa curve, rapid expansion upon melting takes place. As expected, an increase in applied load leads to smaller actuation strains. At 10 kPa load, the CNT−paraffin nanocomposite collapses after melting, which suggests that the

DOI: 10.1021/acsami.5b01141
ACS Appl. Mater. Interfaces 2015, 7, 8218−8224

blocking stress of the CNT−paraffin actuator in regime 2 (above the wax melting point) is between 1 and 10 kPa. In the shown data for regime 2, the strains reached under load slightly surpass those reached in the no load condition, which is likely due to run-to-run variation in CNT forest density.[21]

Once the wax is melted inside the CNT forest (>60 °C), the vertical stiffness of the film decreases significantly, as shown in Figure 3. This signifies the onset of regime 2. The reported

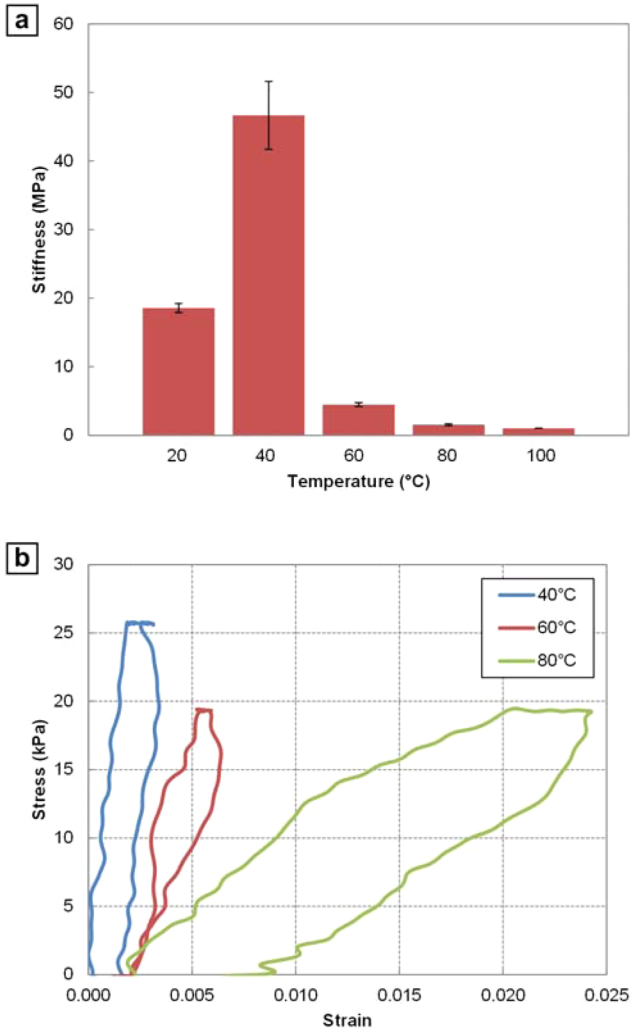

Figure 3. (a) Temperature dependent compressive stiffness of CNT−paraffin films and (b) exemplary stress−strain curves used to determine stiffness.

stiffness is calculated from the initial positive slopes of each stress−strain curve during the unloading. At room temperature, the modulus of the actuator is 18.6 MPa, which is approximately 15-fold greater than a corrugated (crushed) CNT forest that has not been infiltrated with paraffin. The actuator stiffness unexpectedly increases to 46.7 MPa at 40 °C. The actuator stiffness then drops significantly, to 4.5 MPa, as the wax melts at 60 °C, while at 100 °C, the stiffness of the actuator drops to 1.2 MPa, which is less than the stiffness of the corrugated CNTs without paraffin.

A similar pure paraffin wax would be expected to undergo a solid−solid phase transition just below the melting point (47.0−53.3 °C).[22,23] The phases and transition points depend on the chain length, amounts and types of impurities, and external pressure.[23] In general, within this temperature range, paraffin wax transition to a softer phase where molecules are free to rotate about their chain axis prior to melting. Because an increase in pressure is expected to move the transition point closer to the melting point and because the majority of the actuation in regime 1 takes place significantly below the wax melting point, we do not expect that the solid−solid phase transition is responsible for the observed actuation.

Instead, actuation of the CNT−paraffin film in regime 1 is likely powered by the release of the deformation energy (stored in the CNTs during wax freezing), which does work against the viscous forces in the wax and lifts the applied load upward by up to 3% strain at 10 kPa. Because the compressive load used to crush the forest is maintained during cooling of the freshly infiltrated wax and because wax undergoes shrinkage during cooling, additional elastic energy is stored in the CNT network during freezing of the wax. As the wax softens before melting, it allows the corrugated microstructure to relax, releasing the stored deformation energy. When the wax melts, the wavelength of the corrugated CNT morphology increases, signaling the onset of regime 2. The behavior of the composite in regime 1, below the wax melting point, is analogous to some shape memory materials, where elastic deformation energy is first stored at lowered temperatures and is later released during heating, resulting in a shape change. However, unlike most shape memory materials, upon subsequent cooling, the wax pulls the CNTs back to their initial corrugated shape without requiring an external restoring force. Therefore, the CNT−paraffin system is a fully reversible shape memory composite, and to our knowledge, this is the first time that such has been achieved using paraffin wax as the active material. The observed behavior has similarities to shape memory materials exhibiting an intrinsic two-way effect.

In regime 2, the wax has undergone melting and expands up to 20% more in total, doing work to extend the corrugated CNT forest. The equilibrium position of the actuator, at elevated temperature, is reached when pressure of the molten wax inside the forest equals the pressure required to incrementally extend the forest in the vertical direction in addition to any externally applied load. If the pressure exerted by the paraffin exceeds the capillary pressure, the molten wax is expected to flow out of the forest. For example, loading an actuator to 100 kPa at 150 °C results in the escape of wax, and the film becomes compressed to less than 10% of its initial height.

The actuation properties of CNT−paraffin films are strongly dependent on the compression strain applied to the CNT forest before and during paraffin infiltration; we found that samples compressed by approximately 50% of their initial height resulted in the actuators with the largest vertical stroke (Figure S4, Supporting Information). When compressed by 50% of its as-grown thickness, a CNT forest was observed to have a corrugated conformation for the lower 45−50% of its compressed thickness (as viewed from the side). Further, the density and alignment of the CNTs within the forest are expected to influence the capillary pressure confining the wax within the composite, therefore changing the actuator stiffness and strain output. A greater CNT density would result in a lower average spacing between individual CNTs, resulting in a greater capillary pressure of the paraffin and therefore a greater blocking stress of the actuator. Additionally, we expect that a greater CNT forest density will correspond to greater actuator stiffness at the expense of less maximum strain. For regime 2,

DOI: 10.1021/acsami.5b01141
ACS Appl. Mater. Interfaces 2015, 7, 8218−8224

this trade-off is due to the energy density of the process powering the shape change, in this case, the phase transition and thermal expansion of paraffin, remaining largely unchanged by the density, morphology, or increased stiffness of the CNT forests.

While the CNT−paraffin actuators exert a relatively low stress after melting (<10 kPa), they exert an impressive force of 176 mN with a total actuator footprint of only 0.32 cm^2. This is because the wax is efficiently confined within the CNT forest, which occupies less than 1% of the total volume. The maximum actuation strain of the CNT−paraffin nanocomposite (~0.02−0.2) exceeds that of shape memory alloys (~0.07)[3] and approaches that of natural muscle (~0.3−0.7).[3] Further study is needed to explore the mechanism and limits of actuation, yet it is clear that the strain and stress will be related to the density of the CNTs, their initial deformation, and the intrinsic active behavior of the paraffin wax. Moreover, although the blocking stress for regime 1 is not known, the present CNT−paraffin film actuator is able to lift at least 2000 times its weight (8.7 mg of paraffin) at 40 °C. The largest measured specific work for our actuator in regime 1 (below the wax melting point) is 846 J/kg, while the maximum specific work produced in regime 2 is only 342 J/kg. The specific work in regime 2 is limited by the low blocking force. On the basis of the CNT−paraffin actuator stiffness in regime 1 and the measured strain, the blocking stress for this regime is predicted to be 1.4 MPa. This is comparable to paraffin actuators wherein the wax is sealed in a container and undergoes melting.[1] A comparison of the CNT−paraffin film performance to traditional actuators and active materials can be found in Figure S6 of the Supporting Information.

Last, we explore one potential application of the CNT−paraffin film actuator, a passive thermal switch,[24] which enables engineered heat dissipation via self-actuated contact with a second surface. We present a preliminary demonstration of this by measuring the thermal conductivity of the CNT−paraffin actuator as it expands upward to contact a second surface. We constructed a setup with thin film heat flux sensors on parallel surfaces (Figure 4A) and then measured heat flux through the composite versus temperature as it closes the gap between the surfaces (Figure 4B). The thermal conductivity of the CNT−paraffin composite was calculated from a combined thermal resistance model using the measured heat flux into the heat sink and the temperature difference between the hot plate and the heat sink (see Supporting Information for model description).

When the system is heated from below the CNT−paraffin film, the thermal resistance is initially large, while most of the heat is absorbed by the paraffin wax. As the film expands, the thermal resistance of the actuator and the gap decreases rapidly, the air gap is reduced, the conductivity of the paraffin increases,[25] and ultimately the actuator contacts the heat sink. As the gap closes and the composite contacts the upper heat sink, the thermal conductivity increases to approximately 0.4 W/m-K at 70 °C (Figure S5, Supporting Information). This value is approximately twice that of neat high thermal conductivity paraffin wax at room temperature (0.21−0.24 W/m-K) and approximately three times that of a paraffin wax with comparable molecular weight at 70 °C (0.13 W/m-K).[26] The greater thermal conductivity than neat paraffin is due to the presence of aligned CNTs within the composite (~1 wt %). Further enhancement in composite thermal conductivity may be gained by inclusion of graphite nanoplatelets in the paraffin; a recent study showed that 7 wt % graphene increased thermal

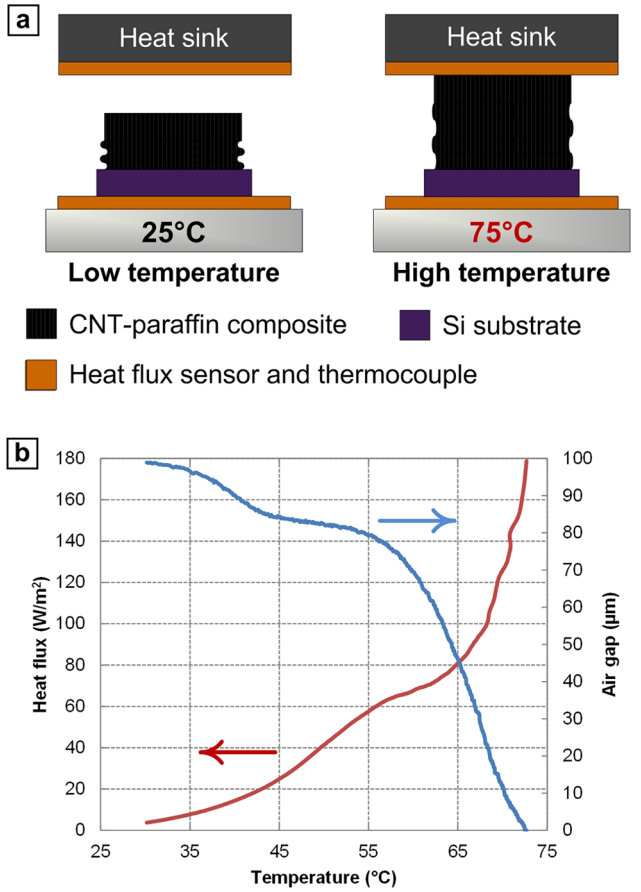

Figure 4. Demonstration of CNT−paraffin actuator as a passive thermal switch. (a) Simplified setup of measurement configuration; (b) measured heat flux through the actuator versus gap between the surfaces.

conductivity from 0.25 to 0.85W/m-K.[27] The final value is comparable to commercially available polymer−ceramic composite thermal transfer tapes[28] and is close to that of passive composites made by polymer infiltration to CNT forests.[29,30] In principle, the temperature at which the actuator engages the heat sink could be controlled via the initial gap or the physical characteristics of the CNT−paraffin film (prestrain, paraffin composition, CNT density, etc.). We expect this degree of engineering to be broadly useful for thermally responsive surfaces, which are useful in modulating flow control, wetting, optical, and thermal properties.

CONCLUSION

In summary, we have shown that large-stroke microstructured thermal actuators can be made by infiltration of corrugated CNT forests with paraffin wax. Two fundamentally distinct mechanistic regimes of the CNT−paraffin actuator were identified: (1) a reversible shape memory behavior regime with high stiffness and low strain below the melting point and (2) a low stiffness, high strain regime above the melting point. In regime 1, the actuator was capable of lifting 2000 times is own weight (exerting and impressive force of 176 mN) with an actuation strain of 3% and a stress of 10 kPa at 40 °C, while in regime 2, the actuator was shown to reach an actuation strain of 20% and a stress of 1 kPa at 175 °C. This large-stroke vertical actuation is enabled by strong capillary interaction between paraffin and CNTs, and engineering of the vertical compliance

DOI: 10.1021/acsami.5b01141
ACS Appl. Mater. Interfaces 2015, 7, 8218−8224

by corrugation of the CNT forest on the microscale. CNT–paraffin nanocomposites have been shown to act as switchable thermal interfaces with a thermal conductivity up to 0.4 W/m-K at 70 °C with a CNT content of 1 wt %. Because the CNT–paraffin film actuators do not require external confinement to restrain the wax, the materials are amenable to integration with laminates and miniaturization for applications including thermally responsive surfaces and flow control.

■ ASSOCIATED CONTENT

Supporting Information

Detailed experimental procedures, video of actuation, actuation strain dependence on CNT forest precompression, actuator performance comparison, and thermal conductivity model. This material is available free of charge via the Internet at http://pubs.acs.org.

■ AUTHOR INFORMATION

Corresponding Author

*E-mail: ajhart@mit.edu.

Present Address

†Department of Engineering, Institute for Manufacturing, University of Cambridge, 17 Charles Babbage, Cambridge CB3 0FS, U.K.

Notes

The authors declare no competing financial interest.

■ ACKNOWLEDGMENTS

Primary financial support was provided by the Air Force Office of Scientific Research Young Investigator Program (FA9550-11-1-0089). The force control system and imaging apparatus was originally built for a project funded by the Department of Energy Office of Basic Energy Sciences (DE-SC0004927). We thank Justin Beroz, Mostafa Bedewy, Kendall Teichert, Ryan Oliver, and Tom Serbowicz for contributions to the design and fabrication of the force control and imaging systems. Microfabrication was performed at the Lurie Nanofabrication Facility (LNF), which is a member of the National Nanotechnology Infrastructure Network (NNIN), and electron microscopy was performed at the Electron Microbeam Analysis Laboratory (EMAL), both at the University of Michigan.

■ REFERENCES

(1) Kabei, N.; Kosuda, M.; Kagamibuchi, H.; Tashiro, R.; Mizuno, H.; Ueda, Y.; Tsuchiya, K. A Thermal-Expansion-Type Microactuator with Paraffin as the Expansive Material: Basic Performance of a Prototype Linear Actuator. *JSME Int. J., Ser. C* **1997**, *40*, 736–742.

(2) Carlen, E. T.; Mastrangelo, C. H. Electrothermally Activated Paraffin Microactuators. *J. Microelectromech. Syst.* **2002**, *11*, 165–174.

(3) Huber, J. E.; Fleck, N. A.; Ashby, M. F. The Selection of Mechanical Actuators. *Proc. R. Soc. London, Ser. A* **1997**, *453*, 2185–2205.

(4) Bodén, R.; Lehto, M.; Simu, U.; Thornell, G.; Hjort, K.; Schweitz, J.-Å. A Polymeric Paraffin Actuated High-Pressure Micropump. *Sens. Actuators, A* **2006**, *127*, 88–93.

(5) Selvaganapathy, P.; Carlen, E. T.; Mastrangelo, C. H. Electrothermally Actuated Inline Microfluidic Valve. *Sens. Actuators A* **2003**, *104*, 275–282.

(6) Carlen, E. T.; Edwin, T.; Mastrangelo, C. H. C. H. Surface Micromachined Paraffin-Actuated Microvalve. *J. Microelectromech. Syst.* **2002**, *11*, 408–420.

(7) Boustheen, A.; Homburg, F. G. A.; Somhorst, M. G. A. M.; Dietzel, A. A Layered Modular Polymeric M-Valve Suitable for Lab-on-Foil: Design, Fabrication, and Characterization. *Microfluid. Nanofluid.* **2011**, *11*, 663–673.

(8) Yang, B.; Lin, Q. A Latchable Microvalve Using Phase Change of Paraffin Wax. *Sens. Actuators, A.* **2007**, *134*, 194–200.

(9) Thornell, L. K.; G. A Thermal Microactuator Made by Partial Impregnation of Polyimide with Paraffin. *J. Micromech. Microeng.* **2002**, *12*, 849.

(10) Lehto, M.; Bodén, R.; Simu, U. A Polymeric Paraffin Microactuator. *J. Microelectromech. Syst.* **2008**, *17*, 1172–1177.

(11) Ogden, S.; Klintberg, L.; Thornell, G.; Hjort, K.; Bodén, R. Review on Miniaturized Paraffin Phase Change Actuators, Valves, and Pumps. *Microfluid. Nanofluid.* **2013**, *17*, 53–71.

(12) Lima, M. D.; Li, N.; Jung de Andrade, M.; Fang, S.; Oh, J.; Spinks, G. M.; Kozlov, M. E.; Haines, C. S.; Suh, D.; Foroughi, J.; Kim, S. J.; Chen, Y.; Ware, T.; Shin, M.; Machado, L. D.; Fonseca, A. F.; Madden, J. D. W.; Voit, W. E.; Galvão, D. S.; Baughman, R. H. Electrically, Chemically, and Photonically Powered Torsional and Tensile Actuation of Hybrid Carbon Nanotube Yarn Muscles. *Science* **2012**, *338*, 928–932.

(13) Chun, K.-Y.; Hyeong Kim, S.; Kyoon Shin, M.; Hoon Kwon, C.; Park, J.; Tae Kim, Y.; Spinks, G. M.; Lima, M. D.; Haines, C. S.; Baughman, R. H.; Kim, S. J. Hybrid Carbon Nanotube Yarn Artificial Muscle Inspired by Spider Dragline Silk. *Nat. Commun.* **2014**, *5*, 3322.

(14) Hart, A. J.; Slocum, A. H. Rapid Growth and Flow-Mediated Nucleation of Millimeter-Scale Aligned Carbon Nanotube Structures from a Thin-Film Catalyst. *J. Phys. Chem. B* **2006**, *110*, 8250–8257.

(15) Copic, D.; Park, S. J.; Tawfick, S.; De Volder, M.; Hart, A. J. Fabrication, Densification, and Replica Molding of 3D Carbon Nanotube Microstructures. *J. Visualized Exp.* **2012**, *65*, No. e3980.

(16) Cao, A.; Dickrell, P. L.; Sawyer, W. G.; Ghasemi-Nejhad, M. N.; Ajayan, P. M. Super-Compressible Foamlike Carbon Nanotube Films. *Science* **2005**, *310*, 1307–1310.

(17) Hutchens, S. B.; Needleman, A.; Greer, J. R. A Microstructurally Motivated Description of the Deformation of Vertically Aligned Carbon Nanotube Structures. *Appl. Phys. Lett.* **2012**, *100*, 121910.

(18) Pour Shahid Saeed Abadi, P.; Hutchens, S. B.; Greer, J. R.; Cola, B. A.; Graham, S. Buckling-Driven Delamination of Carbon Nanotube Forests. *Appl. Phys. Lett.* **2013**, *102*, 223103.

(19) Pathak, S.; Mohan, N.; Decolvenaere, E.; Needleman, A.; Bedewy, M.; Hart, A. J.; Greer, J. R. Failure and Strength in Vertically Aligned Carbon Nanotubes. *ACS Nano* **2013**, *7*, 8593–8604.

(20) Simha, R.; Wilson, P.; Olabisi, O. Pressure–Volume–Temperature Properties of Amorphous Polymers: Empirical and Theoretical Predictions. *Kolloid Z. Z. Polym.* **1973**, *251*, 402–408.

(21) Oliver, C. R.; Polsen, E. S.; Meshot, E. R.; Tawfick, S.; Park, S. J.; Bedewy, M.; Hart, A. J. Statistical Analysis of Variation in Laboratory Growth of Carbon Nanotube Forests and Recommendations for Improved Consistency. *ACS Nano* **2013**, *7*, 3565–3580.

(22) Schaerer, A. A.; Busso, C. J.; Smith, A. E.; Skinner, L. B. Properties of Pure Normal Alkanes in the C 17 to C 36 Range. *J. Am. Chem. Soc.* **1955**, *77*, 2017–2019.

(23) Broadhurst, M. G. An Analysis of the Solid Phase Behavior of the Normal Paraffins. *J. Res. Natl. Bur. Stand., Sect. A* **1962**, *66A* (No. 3), 241–249.

(24) Geng, X.; Patel, P.; Narain, A.; Meng, D. D. A Self-Adaptive Thermal Switch Array for Rapid Temperature Stabilization under Various Thermal Power Inputs. *J. Micromech. Microeng.* **2011**, *21*, 085018.

(25) Sarı, A.; Karaipekli, A. Thermal Conductivity and Latent Heat Thermal Energy Storage Characteristics of Paraffin/Expanded Graphite Composite as Phase Change Material. *Appl. Therm. Eng.* **2007**, *27*, 1271–1277.

(26) Kenisarin, M. M. Thermophysical Properties of Some Organic Phase Change Materials for Latent Heat Storage. A Review. *Sol. Energy* **2014**, *107*, 553–575.

(27) Kim, S.; Drzal, L. T. High Latent Heat Storage and High Thermal Conductive Phase Change Materials Using Exfoliated Graphite Nanoplatelets. *Sol. Energy Mater. Sol. Cells* **2009**, *93*, 136–142.

DOI: 10.1021/acsami.5b01141
ACS Appl. Mater. Interfaces 2015, 7, 8218–8224

(28) *Thermally Conductive Adhesive Transfer Tapes 8805 • 8810 • 8815 • 8820*; 3M Electronics: St. Paul, MN, 2008.
(29) Marconnet, A. M.; Yamamoto, N.; Panzer, M. a; Wardle, B. L.; Goodson, K. E. Thermal Conduction in Aligned Carbon Nanotube−Polymer Nanocomposites with High Packing Density. *ACS Nano* **2011**, *5*, 4818−4825.
(30) Cola, B. A.; Hodson, S. L.; Xu, X.; Fisher, T. S. Carbon Nanotube Array Thermal Interfaces Enhanced With Paraffin Wax. *Proc. ASME Summer Heat Transfer Conf., 2008* **2008**, 765−770.

NOTE ADDED AFTER ASAP PUBLICATION

This paper was published on the Web on April 8, 2015, with minor text errors in the Abstract. The corrected version was reposted on April 9, 2015.

DOI: 10.1021/acsami.5b01141
ACS Appl. Mater. Interfaces 2015, 7, 8218−8224